

## DISC TOOL PROFILING – A COMPARISON BETWEEN CAD METHOD AND ANALYTICAL METHOD

**Gabriel FRUMUȘANU<sup>1,\*</sup>, Silviu BERBINSCHI<sup>2</sup>, Nicolae OANCEA<sup>3</sup>**

<sup>1)</sup> Prof., PhD, Manufacturing Science & Engineering Department, “Dunărea de Jos” University, Galați, Romania

<sup>2)</sup> Assist., Manufacturing Science & Engineering Department, “Dunărea de Jos” University, Galați, Romania

<sup>3)</sup> Prof., PhD, Manufacturing Science & Engineering Department, “Dunărea de Jos” University, Galați, Romania

**Abstract:** *In this paper, there are suggested solutions for profiling the disc tool reciprocal enwrapped to a helical cylindrical surface, with constant pitch. A graphical method has been developed in CATIA environment together with an analytical one, on the base of the helical motion decomposition theorem. There are presented solutions for the disc tool axial section in both analytical and graphical form. There are also included numerical examples concerning the same surface, in order to prove the quality of the graphical method when it is used in profiling disc tools, which generate through enveloping.*

**Key words:** *disc-tool profiling, CAD method, analytical method, helical cylindrical surface, helical motion decomposition.*

### 1. INTRODUCTION

Helical cylindrical surfaces with constant pitch are encountered in practice as helical slots on the active surfaces of different parts (helical screws, worms, helical teeth gears, helical pumps components etc.) or cutting tools (helical drills, helical teeth reamers, helical counterbores, cylindrical mills with helical teeth). To generate this kind of surface involves solving a specific problem: to find the contact conditions and the corresponding characteristic curve, at the contact between a helical cylindrical surface with constant pitch and the tool primary peripheral surface (generated by the cutting edge during the cutting motion around the disc-tool axis).

There are known analytical solutions for profiling the tools that generates by enwrapping, based on the embraced surfaces fundamental theorems – Olivier first theorem [1], Gohman theorem [1 and 2]. Nikolaev theorem [8 and 11] it is also frequently used, by decomposing the helical motion in rotation motions (or in rotation and translation motions). Moreover, analytical methods complementary to the fundamental ones were developed – the minimum distance method [10], the plain generating trajectories method [12].

Solutions to profile the tools used for generating helical surfaces were suggested by approximating the helical surface generator line through Bézier polynomial functions [6 and 13]. This way, by knowing only a limited number of points along the generated profile, it is possible to find with acceptable precision (from technical point of view) the required active profiles of the cutting tools delimited by revolution primary peripheral surfaces.

The graphic designing environments development enabled the elaboration of dedicated methods and soft products for solving the problematic concerning the helical surfaces generation, by solid modeling [3–5, 7, 9], leading to rigorous and suggestive solutions. From this category, CATIA environment opens a new way to approach the enounced problematic, which will be further developed in this paper. The new method quality will be assessed by making a comparison between the results of its application and those obtained by using an analytical method.

### 2. DISC-TOOL PROFILING

The generating process kinematics, in the case of a helical surface and by using a tool delimited by a revolution primary peripheral surface – a disc-tool – involves a combination of three motions (see Fig. 1):

I – rotation motion of the worked piece on which the helical surface to be generated (cylindrical and having constant pitch) is placed;

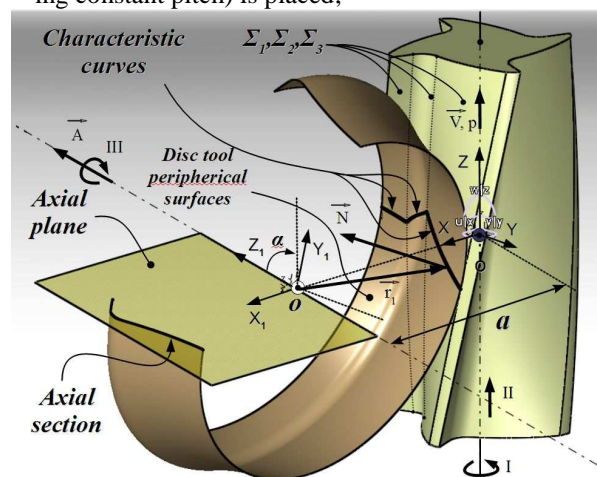


**Fig. 1.** Disc-tool primary peripheral surface and helical surface to be generated (composite surface).

\* Corresponding author: “Dunărea de Jos” University, Manufacturing Science & Engineering Department, Domnească str. 111, 800201 – Galați, Romania, <http://www.tcm.ugal.ro>  
 E-mail addresses: [gabriel.frumusanu@ugal.ro](mailto:gabriel.frumusanu@ugal.ro) (G. Frumușanu), [silviu.berbinschi@ugal.ro](mailto:silviu.berbinschi@ugal.ro) (S. Berbinschi), [nicolae.oancea@ugal.ro](mailto:nicolae.oancea@ugal.ro) (N. Oancea)

II – translation motion along the worked piece rotation axis, correlated to the rotation motion, having as purpose to create a helical motion of  $\vec{V}$  axis and  $p$  parameter identical to the generated surface ones;

III – cutting motion – tool rotation around its axis,  $\vec{A}$ .

The following reference systems have to be considered:

- $XYZ$ , meaning a system attached to the helical surface to be generated, having the  $Z$  axis coincident to  $\vec{V}$  axis of the helical surface.
- $X_1Y_1Z_1$  – system attached to the disc-tool axis,  $\vec{A}$ .

Nikolaev theorem applied in order to find the characteristic curve owing to both surfaces,  $\Sigma$ , to be generated and  $S$  – tool primary peripheral surface is (see also Fig. 1)

$$(\vec{A}, \vec{N}_\Sigma, \vec{r}_i) = 0, \quad (1)$$

where:  $\vec{A}$  is the vector of the disc-tool surface  $S$  rotation axis;

$\vec{N}_\Sigma$  –  $\Sigma$  surface normal, into the  $XYZ$  system;

$\vec{r}_i$  – the position vector of the current point from  $\Sigma$  surface, referred to  $X_1Y_1Z_1$  origin,  $O_1$ .

The relation (1) shows that the contact (tangency) points between  $\Sigma$  and  $S$  surfaces mean, in fact, the intersection points between the normal lines laid from the  $\vec{A}$  ( $Z_1$ ) axis points onto  $\Sigma$  surface, hence the  $\vec{A}$  axis projection onto  $\Sigma$  surface.

We consider that the surface  $\Sigma$  equations are:

$$\begin{cases} X = X(u, v); \\ \Sigma Y = Y(u, v); \\ Z = Z(u, v), \end{cases} \quad (2)$$

where  $u$  and  $v$  are independent, variable parameters.

The vectors from relation (1) are defined as:

$$\vec{A} = \cos \alpha \cdot \vec{j} - \sin \alpha \cdot \vec{k}, \quad (3)$$

$$\vec{r}_i = [X(u, v) - a] \cdot \vec{i} + Y(u, v) \cdot \vec{j} + Z(u, v) \cdot \vec{k}, \quad (4)$$

$$\vec{N}_\Sigma = \begin{vmatrix} \vec{i} & \vec{j} & \vec{k} \\ \dot{X}_u & \dot{Y}_u & \dot{Z}_u \\ \dot{X}_v & \dot{Y}_v & \dot{Z}_v \end{vmatrix}. \quad (5)$$

The surface  $\Sigma$  can be effectively determined on the base of condition (1) which, in fact, means a relation of the type

$$q(u, v) = 0, \quad (6)$$

or explicit

$$u = u(v). \quad (7)$$

The Eqs. (2) together to relation (7) give the equations of the characteristic curve, on the surface  $\Sigma$ :

$$C_\Sigma \begin{cases} X = X(v); \\ Y = Y(v); \\ Z = Z(v). \end{cases} \quad (8)$$

The curve  $C_\Sigma$  can be determined with the help of CATIA designing environment facilities, which, at “*Projection*” command, enable to project the  $\vec{A}$  axis onto the  $\Sigma$  surface; this way, the points constituting the characteristic can be expressed through a matrix of points, equivalent to the equations (8),

$$C_\Sigma = \begin{pmatrix} X_1 & Y_1 & Z_1 \\ X_2 & Y_2 & Z_2 \\ \vdots & \vdots & \vdots \\ X_n & Y_n & Z_n \end{pmatrix}. \quad (9)$$

If “ $n$ ” (the number of points from the matrix of above) is high enough, the precision in finding the characteristic curve could be adequate to the technical requirements concerning the design of the disc-tool reciprocal enwrapped to a helical surface.

By using the co-ordinates transform

$$\begin{pmatrix} X_1 \\ Y_1 \\ Z_1 \end{pmatrix} = \begin{pmatrix} 1 & 0 & 0 \\ 0 & \cos \alpha & -\sin \alpha \\ 0 & \sin \alpha & \cos \alpha \end{pmatrix} \cdot \begin{bmatrix} X \\ Y \\ Z \end{bmatrix} - \begin{pmatrix} a \\ 0 \\ 0 \end{pmatrix} \quad (10)$$

the characteristic curve co-ordinates are transferred, in (8) or (9) form, to  $X_1Y_1Z_1$  system:

$$C_{\Sigma_{X_1Y_1Z_1}} = \begin{pmatrix} X_{11} & Y_{11} & Z_{11} \\ X_{12} & Y_{12} & Z_{12} \\ \vdots & \vdots & \vdots \\ X_{1n} & Y_{1n} & Z_{1n} \end{pmatrix}. \quad (11)$$

Finally, the disc-tool axial section result from (11) as

$$S_A \begin{cases} R = \sqrt{X_{1i}^2 + Y_{1i}^2}; \\ H = Z_{1i}, \end{cases} \quad i = 1, 2, \dots, n. \quad (12)$$

### 3. 3-D METHOD TO PROFILE THE DISC-TOOL

The 3-D method to profile the disc-tool – *HSGT* (**H**elical **S**urface **G**enerating **T**ool) is grounded on the Generative Shape Design environment facilities. The worked piece (in fact, the generated surface) is 3-D modeled, as it can be observed in Fig. 2 (the case of a circular transversal profile) or in Fig. 3 (the case of a rectilinear transversal profile).

The worked piece reference system,  $XYZ$  and the disc-tool reference system,  $X_1Y_1Z_1$ , the last one as Euler system are created (see Figs. 2 and 3).

By giving the “*Projection*” command, the disc-tool axis projection onto the  $\Sigma$  surface is realized; thus, the characteristic curve is determined.

By subsequently using the “*Revolve*” command, the tool primary peripheral surface –  $S$  results, after rotating the characteristic curve around  $Z_1$  axis.

The disc-tool axial section is then obtained as intersection between the surface  $S$  and a plain which includes the  $Z_1$  ( $\vec{A}$ ) axis – by applying the “*Intersection*” command.

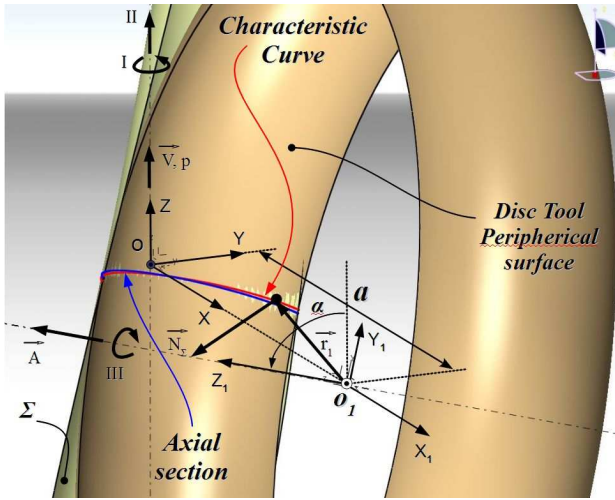


Fig. 2. Worked piece 3D model (circular transversal profile).

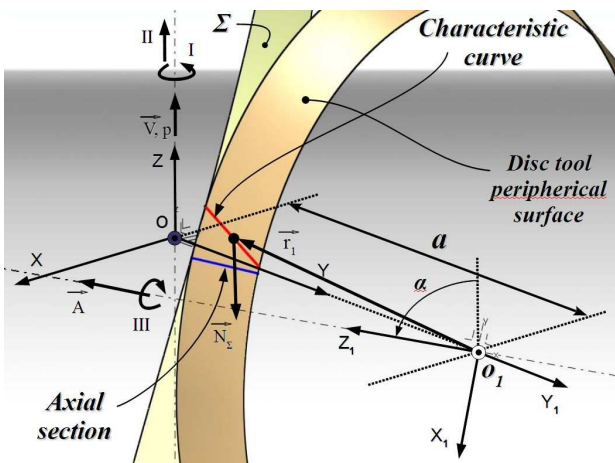


Fig. 3. Worked piece 3D model (rectilinear transversal profile).

#### 4. COMPARISON BETWEEN THE CAD METHOD AND THE ANALYTICAL METHOD

We further make a comparison between the results obtained when profiling the disc-tool if using two different methods (CAD, respectively analytical), in order to assess the CAD method performance. Two cases were considered – circular and rectilinear generator curves – and they are both referring to a helical cylindrical surface of constant pitch.

##### 4.1. Helical surface with circular generating curve in frontal plain

The shape of the frontal generating curve of the helical surface to be generated is shown in Fig. 4. The arc of circle has its center in  $O_C [X_{Oc}, Y_{Oc}]$  and passes through the points  $A [X_A, Y_A]$  and  $B [X_B, Y_B]$ . Its equations are:

$$\begin{cases} X = X_{Oc} - r \cos \theta; \\ Y = Y_{Oc} + r \sin \theta, \end{cases} \quad (13)$$

where  $\theta$  is a variable parameter and

$$r = \sqrt{(X_A - X_{Oc})^2 + (Y_A - Y_{Oc})^2} = \sqrt{(X_B - X_{Oc})^2 + (Y_B - Y_{Oc})^2} \quad (14)$$

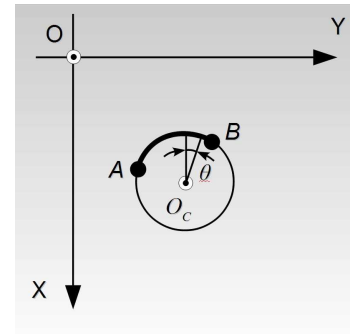


Fig. 4. The frontal circular generating curve.

The helical surface of  $Z (\vec{V})$  axis and  $p$  parameter has the equations:

$$\begin{cases} X = [X_{Oc} - r \cos \theta] \cos \varphi - [Y_{Oc} + r \sin \theta] \sin \varphi; \\ Y = [X_{Oc} - r \cos \theta] \sin \varphi + [Y_{Oc} + r \sin \theta] \cos \varphi; \\ Z = p \cdot \varphi. \end{cases} \quad (15)$$

The normal to the  $\Sigma$  surface has, in the  $XY$  plain, the following components:

$$\begin{aligned} N_x &= -p \cos(\theta - \varphi); \\ N_y &= p \sin(\theta - \varphi); \\ N_z &= -\cos(\theta - \varphi) \{ [X_{Oc} - r \cos \theta] \sin \varphi + [Y_{Oc} + r \sin \theta] \cos \varphi \} \\ &\quad - \sin(\theta - \varphi) \{ [X_{Oc} - r \cos \theta] \cos \varphi + [Y_{Oc} + r \sin \theta] \sin \varphi \}. \end{aligned} \quad (16)$$

The angular parameter  $\alpha$  (from (3)) is defined as

$$\alpha = \arctan\left(\frac{p}{R_e}\right), \quad (17)$$

where  $R_e$  means the worked piece exterior radius.

The vector  $\vec{r}_1$  from (4) becomes

$$\begin{aligned} \vec{r}_1 &= \{ [X_{Oc} - r \cos \theta] \cos \varphi - [Y_{Oc} + r \sin \theta] \sin \varphi - a \} \cdot \vec{i} + \\ &\quad + \{ [X_{Oc} - r \cos \theta] \sin \varphi - [Y_{Oc} + r \sin \theta] \cos \varphi \} \cdot \vec{j} + p \cdot \varphi \cdot \vec{k}. \end{aligned} \quad (18)$$

The enveloping condition can now be written as:

$$q = \begin{vmatrix} N_x & N_y & N_z \\ 0 & -\sin \alpha & \cos \alpha \\ r_{1x} & r_{1y} & r_{1z} \end{vmatrix} \leq \varepsilon, \quad (19)$$

where  $\varepsilon$  is small enough ( $10^{-3} \dots 10^{-5}$ ).

The ensemble formed by Eqs. (15) and condition (19) determines, at a discrete variation of the parameter  $\varphi$ , the co-ordinates of the points along the characteristic curve,

$$C_\Sigma = \begin{pmatrix} X_i \\ Y_i \\ Z_i \end{pmatrix}^T, \quad i = 1, 2, \dots, n. \quad (20)$$

By applying a co-ordinates transform,

$$\begin{aligned} X_{1i} &= X_i - a; \\ Y_{1i} &= Y_i \cos \alpha + Z_i \sin \alpha; \\ Z_{1i} &= -Y_i \sin \alpha + Z_i \cos \alpha, \end{aligned} \quad (21)$$

the co-ordinates of the points from the characteristic curve are transferred into the  $X_1Y_1Z_1$  system, finding this way the disc-tool transversal section (see (12)).

**Numerical application.** The characteristic curve and the disc-tool axial section were determined in the following example:

- co-ordinates of the given points –  $A[10; -8]; B[10; 8]; O_c[12; 0]$ , expressed in mm;
- the distance,  $a = 40$  mm;
- helical surface pitch,  $p_e = 310$  mm;
- work piece exterior radius,  $R_e = 12$  mm;
- number of points on the tool profile,  $n = 100$ ;
- maximum admissible error,  $\epsilon = 0.001$ .

In Table 1, the characteristic curve points co-ordinates are presented found by using the two methods (3-D versus analytical), in the considered example, while in Fig. 5 and Table 2 – the aspect of the characteristic curve and the co-ordinates of its points.

Table 1

Characteristic curve points co-ordinates [mm]

| Point crt. no. | 3-D method |         |         | Analytical method |         |         |
|----------------|------------|---------|---------|-------------------|---------|---------|
|                | X          | Y       | Z       | X                 | Y       | Z       |
| 1              | 10.2558    | -7.6692 | 1.6111  | 10.2558           | -7.6693 | 1.6109  |
| 2              | 10.0381    | -7.6215 | 1.6014  | 10.0391           | -7.6218 | 1.6012  |
| 3              | 9.8227     | -7.5685 | 1.5902  | 9.8235            | -7.5688 | 1.5900  |
| 4              | 9.6083     | -7.5099 | 1.5777  | 9.6093            | -7.5103 | 1.5776  |
| 5              | 9.3956     | -7.4458 | 1.5638  | 9.3967            | -7.4462 | 1.5637  |
| 6              | 9.1847     | -7.3762 | 1.5486  | 9.1858            | -7.3767 | 1.5485  |
| 7              | 8.9757     | -7.3012 | 1.5322  | 8.9767            | -7.3017 | 1.5322  |
| 8              | 8.7689     | -7.2208 | 1.5146  | 8.7697            | -7.2212 | 1.5146  |
| 9              | 8.5643     | -7.1351 | 1.4959  | 8.5649            | -7.1354 | 1.4959  |
| 10             | 8.3620     | -7.0440 | 1.4760  | 8.3624            | -7.0442 | 1.4761  |
| ...            | ...        | ...     | ...     | ...               | ...     | ...     |
| 50             | 3.7545     | -0.1090 | 0.0225  | 3.7546            | -0.1087 | 0.0224  |
| 51             | 3.7545     | 0.1089  | -0.0224 | 3.7546            | 0.1087  | -0.0224 |
| 52             | 3.7609     | 0.3265  | -0.0673 | 3.7609            | 0.3261  | -0.0673 |
| 53             | 3.7736     | 0.5445  | -0.1123 | 3.7735            | 0.5432  | -0.1121 |
| 54             | 3.7926     | 0.7617  | -0.1571 | 3.7924            | 0.7599  | -0.1568 |
| ...            | ...        | ...     | ...     | ...               | ...     | ...     |
| 100            | 10.2558    | 7.6692  | -1.6111 | 10.2559           | 7.6692  | -1.6115 |

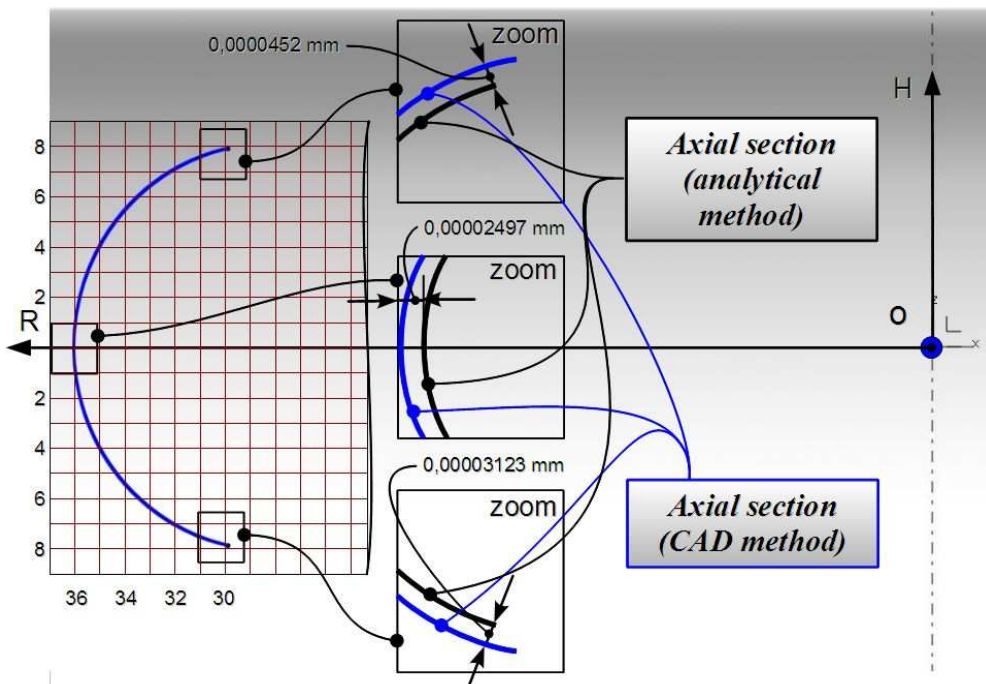


Fig. 5. The tool axial section and the difference between the profiles found by using the two methods.

Table 2  
Axial section points co-ordinates [mm]

| Point crt. no. | 3-D method |         | Analytical method |         |
|----------------|------------|---------|-------------------|---------|
|                | R          | H       | R                 | H       |
| 1              | 29.7451    | 7.8327  | 29.7452           | 7.8327  |
| 2              | 29.9623    | 7.7842  | 29.9619           | 7.7843  |
| 3              | 30.1781    | 7.7300  | 30.1775           | 7.7302  |
| 4              | 30.3926    | 7.6700  | 30.3916           | 7.6704  |
| 5              | 30.6054    | 7.6044  | 30.6043           | 7.6049  |
| 6              | 30.8159    | 7.5334  | 30.8152           | 7.5337  |
| 7              | 31.0248    | 7.4567  | 31.0242           | 7.4570  |
| 8              | 31.2316    | 7.3744  | 31.2312           | 7.3746  |
| 9              | 31.4361    | 7.2867  | 31.4360           | 7.2868  |
| 10             | 31.6386    | 7.1934  | 31.6384           | 7.1935  |
| ...            | ...        | ...     | ...               | ...     |
| 50             | 36.2454    | 0.1112  | 36.2454           | 0.1109  |
| 51             | 36.2454    | -0.1112 | 36.2454           | -0.1109 |
| 52             | 36.2390    | -0.3333 | 36.2391           | -0.3328 |
| 53             | 36.2263    | -0.5558 | 36.2265           | -0.5543 |
| 54             | 36.2073    | -0.7775 | 36.2076           | -0.7754 |
| ...            | ...        | ...     | ...               | ...     |
| 100            | 29.7451    | -7.8327 | 29.7451           | -7.8328 |

4.2. Helical surface with rectilinear generating curve in frontal plain

In Fig. 6, it is presented the rectilinear frontal generating line of the helical cylindrical surface with constant pitch.

The generating line equations are:

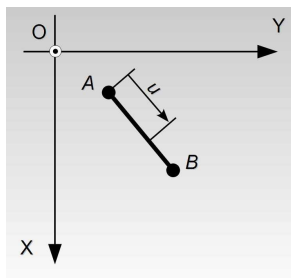


Fig. 6. The frontal rectilinear generating line.

$$\begin{cases} X = X_A + u \cos \theta; \\ Y = Y_A + u \sin \theta, \end{cases} \quad (22)$$

with

$$\theta = \arctan \left( \frac{|Y_B - Y_A|}{|X_B - X_A|} \right) \quad (23)$$

and

$$u_{\min} = 0; u_{\max} = \sqrt{(X_B - X_A)^2 + (Y_B - Y_A)^2} \quad (24)$$

The helical surface equations are, in this case:

$$\begin{cases} X = [X_A + u \cos \theta] \cos \varphi - [Y_A + u \sin \theta] \sin \varphi; \\ \Sigma Y = [X_A + u \cos \theta] \sin \varphi + [Y_A + u \sin \theta] \cos \varphi; \\ Z = p \cdot \varphi, \end{cases} \quad (25)$$

with  $u$  and  $\varphi$  – variable parameters and  $p$  the helical surface parameter.

By proceeding same way as we did in the previous example, after finding the normal  $\vec{N}_z$ , position vector  $\vec{r}_i$  and  $\vec{A}$  vector components and making the substitutions in relation (1), the characteristic curve of  $\Sigma$  surface, embraced with the disc-tool primary peripheral surface, can be determined.

**Numerical application.** The characteristic curve and the disc-tool axial section were determined in the following example:

- coordinates of the given points –  $A[12; -8]; B[16; -2]$ , expressed in mm;
- distance,  $a = 50$  mm;
- helical surface pitch,  $p_e = 310$  mm;
- work piece exterior radius,  $R_e = 15$  mm;
- number of points on the tool profile,  $n = 100$ ;
- maximum admissible error,  $\epsilon = 0.001$ .

In Table 3 there are presented the characteristic curve points co-ordinates found by using the two methods (3-D versus analytical), in the considered example, while in Fig. 6 and Table 4 – the aspect of the characteristic curve and the co-ordinates of its points.

Table 3

Characteristic curve points co-ordinates [mm]

| Point crt. no. | 3-D method |         |        | Analytical method |         |        |
|----------------|------------|---------|--------|-------------------|---------|--------|
|                | X          | Y       | Z      | X                 | Y       | Z      |
| 1              | 13.0353    | -6.1709 | 7.1961 | 13.0353           | -6.1710 | 7.1963 |
| 2              | 13.0587    | -6.1215 | 7.1347 | 13.0588           | -6.1215 | 7.1347 |
| 3              | 13.0824    | -6.0722 | 7.0732 | 13.0825           | -6.0720 | 7.0730 |
| 4              | 13.1061    | -6.0229 | 7.0117 | 13.1063           | -6.0226 | 7.0114 |
| 5              | 13.1300    | -5.9737 | 6.9502 | 13.1303           | -5.9733 | 6.9498 |
| 6              | 13.1541    | -5.9246 | 6.8887 | 13.1544           | -5.9241 | 6.8882 |
| 7              | 13.1783    | -5.8755 | 6.8272 | 13.1787           | -5.8749 | 6.8266 |
| 8              | 13.2026    | -5.8265 | 6.7657 | 13.2030           | -5.8258 | 6.7650 |
| 9              | 13.2271    | -5.7776 | 6.7043 | 13.2276           | -5.7767 | 6.7034 |
| 10             | 13.2517    | -5.7287 | 6.6428 | 13.2523           | -5.7278 | 6.6418 |
| ...            | ...        | ...     | ...    | ...               | ...     | ...    |
| 50             | 14.3534    | -3.8311 | 4.1897 | 14.3557           | -3.8277 | 4.1853 |
| 51             | 14.3838    | -3.7852 | 4.1286 | 14.3862           | -3.7818 | 4.1242 |
| 52             | 14.4144    | -3.7393 | 4.0675 | 14.4168           | -3.7359 | 4.0630 |
| 53             | 14.4451    | -3.6935 | 4.0064 | 14.4475           | -3.6900 | 4.0019 |
| 54             | 14.4760    | -3.6477 | 3.9454 | 14.4784           | -3.6443 | 3.9409 |
| ...            | ...        | ...     | ...    | ...               | ...     | ...    |
| 100            | 16.0425    | -1.6240 | 1.1572 | 16.0425           | -1.6242 | 1.1572 |



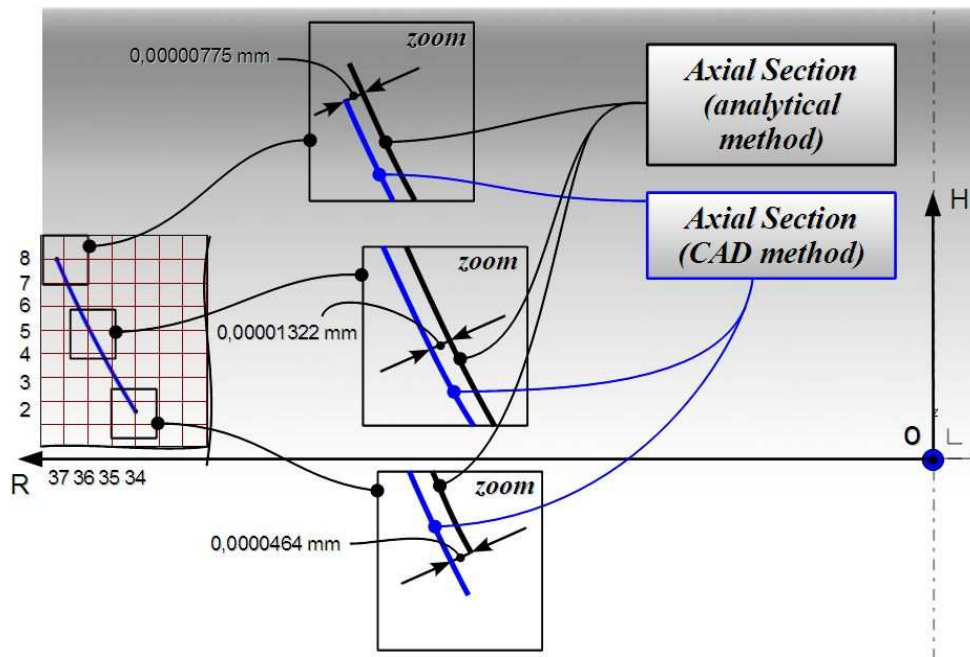


Fig. 6. The tool axial section and the difference between the profiles found by using the two methods.

Table 4  
Axial section points co-ordinates [mm]

| Point crt. no. | 3-D method |        | Analytical method |        |
|----------------|------------|--------|-------------------|--------|
|                | R          | H      | R                 | H      |
| 1              | 37.3134    | 7.9973 | 37.3135           | 7.9974 |
| 2              | 37.2846    | 7.9331 | 37.2841           | 7.9321 |
| 3              | 37.2556    | 7.8689 | 37.2547           | 7.8668 |
| 4              | 37.2265    | 7.8048 | 37.2251           | 7.8017 |
| 5              | 37.1973    | 7.7408 | 37.1954           | 7.7366 |
| 6              | 37.1681    | 7.6769 | 37.1657           | 7.6715 |
| 7              | 37.1387    | 7.6130 | 37.1358           | 7.6066 |
| 8              | 37.1091    | 7.5487 | 37.1058           | 7.5417 |
| 9              | 37.0794    | 7.4848 | 37.0758           | 7.4768 |
| 10             | 37.0497    | 7.4209 | 37.0456           | 7.4120 |
| ...            | ...        | ...    | ...               | ...    |
| 50             | 35.7769    | 4.9081 | 35.7613           | 4.8796 |
| 51             | 35.7430    | 4.8463 | 35.7273           | 4.8179 |
| 52             | 35.7090    | 4.7847 | 35.6933           | 4.7562 |
| 53             | 35.6749    | 4.7230 | 35.6591           | 4.6945 |
| 54             | 35.6407    | 4.6614 | 35.6249           | 4.6330 |
| ...            | ...        | ...    | ...               | ...    |
| 100            | 33.9633    | 1.8904 | 33.9634           | 1.8906 |

## 5. CONCLUSIONS

Two solutions to find the characteristic curve profile when generating a helical surface, by using a disc-tool, were comparatively presented. The graphic 3-D method, developed on the base of an original application HSGT – VBA enables to find the characteristic curve with a very high accuracy. The comparison made to an analytical method, based on the classic Nikolaev theorem, shows a quasi-identity of the results and proves the new 3-D graphical method capacity to be successfully used in solving problems of enwrapped surfaces generation.

## REFERENCES

[1] F.L. Litvin, *Theory of Gearing*, Reference Publication 1212, Nasa, Scientific and Technical Information Division, Washington, D.C., 1984.

- [2] N. Oancea, *Generarea suprafețelor prin înfășurare* (Surfaces generation by enwrapping) Vol. I, Teoreme fundamentale, Edit. Fundației Universitare „Dunărea de Jos” - Galați, 2004.
- [3] N. Oancea, *Generarea suprafețelor prin înfășurare* (Surfaces generation by enwrapping), Vol. II, Teoreme complementare, Editura Fundației Universitare „Dunărea de Jos” – Galați, 2004.
- [4] V. Teodor, N. Oancea, M. Dima, *Profilarea sculelor prin metode analitice* (Tools profiling by analytical methods), Edit. Fundației Universitare „Dunărea de Jos” – Galați, 2006.
- [5] I. Baicu, N. Oancea, *Profilarea sculelor prin modelare solidă* (Cutting tools profiling by solid modeling), Edit. Tehnică – Info, Chișinău, 2002.
- [6] N. Oancea, I. Popa, V. Teodor, V. Oancea, *Tool Profiling for Generation of Discrete Helical Surfaces*, Int. J. of Adv. Manuf. Technol., 2010, 50, pp. 37–46.
- [7] I. Veliko, N. Gentcho, *Profiling of rotation tools for forming of helical surfaces*, Int. J. Mach. Tools Manu., 1998, 38, pp. 1125–1148.
- [8] R.P. Rodin, *Osnovy proektirovaniya rezhushchikh instrumentov* (Basics of design of Cutting Tools), Kiev, Vishcha Shkola, 1990.
- [9] V.G. Shalamanov, S.D. Smentanin, *Shaping of helical surfaces by profiling circles*, Russ. Eng. Res., 2007, 27(7): pp. 470–473, ISSN 1068-798x.
- [10] N. Oancea, *Method numerique pour l’etude des surfaces enveloppees*, Mech. Mach. Theory, 1996, 31(7), pp. 957–972.
- [11] V.S. Lukshin, *Theory of Screw Surfaces in Cutting Tool Design*, Machinostroyeniye, Moscow, 1968.
- [12] V. Teodor, *Contribution to the elaboration of a method for profiling tools – Tools which generate by enwrapping*, Lambert Academie Publishing.
- [13] V.G. Teodor, I. Popa, N. Oancea, *The profiling of end mill and planning tools to generate helical surfaces known by sampled points*, Int. J. Adv. Manuf. Technol, 2010, 51, pp. 439–452.